

*Charged Particles from Capture of Negative Pions by Nuclei*

YU. G. BUDYASHOV, V. G. ZINOV, A. D. KONIN, N. V. RABIN<sup>1)</sup>, AND A. M. CHATRCHYAN<sup>2)</sup>

Joint Institute for Nuclear Research

Submitted August 12, 1971

Zh. Eksp. Teor. Fiz. **62**, 21-30 (January, 1972)

Identification has been made of charged particles emitted on absorption of stopped negative pions by Be, C, Al, S, Ca, Cu, Cd, and Pb of natural isotopic composition. Energy spectra and relative emission probabilities have been measured for protons, deuterons, and tritons, respectively, for energies above 15, 18, and 24 MeV. Estimates are given for the probability of simultaneous emission of two charged particles.

**INTRODUCTION**

ACCORDING to current theoretical ideas and experimental data, direct processes take place in capture of negative pions by nuclei. Absorption of a pion inside a nucleus occurs in a group of a small number of nucleons—a cluster. These clusters may be pp, pn, <sup>3</sup>He, and so forth. Therefore the structure of the nucleus which captures a negative pion should substantially affect the absorption process.

Experimental studies of the energy spectra of charged particles emitted on the absorption of negative pions by nuclei have been carried out by several groups.<sup>[1-4]</sup> However, at the present time the situation is that the accuracy and extent of the experimental data and also the reliability of the theoretical calculations are inadequate to determine uniquely the pion-capture mechanism. Therefore further refinement of previous experimental data, accumulation of new data, and in addition attentive theoretical investigation of the processes of negative-pion capture by nuclei are very desirable.

The purpose of the present work was to measure the relative probabilities of negative-pion capture by nuclei with emission of protons, deuterons, and tritons over a wide range of nuclear charge, to measure the energy spectra of charged particles with energies greater than 15 MeV, and to estimate the fraction of events with simultaneous emission of two charged particles in one pion-capture event.

**EXPERIMENTAL ARRANGEMENT AND APPARATUS**

The work was carried out in the meson beam of the synchrocyclotron at the Laboratory of Nuclear Problems, Joint Institute for Nuclear Research. The 180-MeV/c negative pion beam was used. Measurements were carried out in the nuclei <sup>9</sup>Be, <sup>12</sup>C, <sup>27</sup>Al, <sup>32</sup>S, <sup>40</sup>Ca, <sup>64</sup>Cu, <sup>112</sup>Cd, and <sup>207</sup>Pb. This set of targets permitted the results of the present work to be compared with our earlier study<sup>[5]</sup> of nuclear capture of negative muons.

In order to separate the charged particles according to mass, simultaneous measurements were made of the ionization loss and total energy. Figure 1 shows the ex-

perimental geometry, and Fig. 2 a simplified block diagram of the electronics. The incident pion beam was separated by scintillation counters 1, 2, and 3 and defined by a copper collimator of oval shape. The scintillator of counter 3 was a plastic ellipse with axes 3 cm and 1.5 cm and thickness 300 μ. Targets of thickness

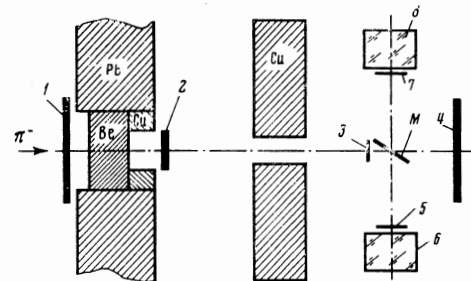


FIG. 1. Diagram of experimental arrangement. 1, 2, 3, 4—scintillation counters; 5, 7—silicon surface-barrier detectors; 6, 8—CsI(Tl) crystal spectrometers; Pb, Cu—collimator system, Be—beryllium absorber, M—interchangeable target.

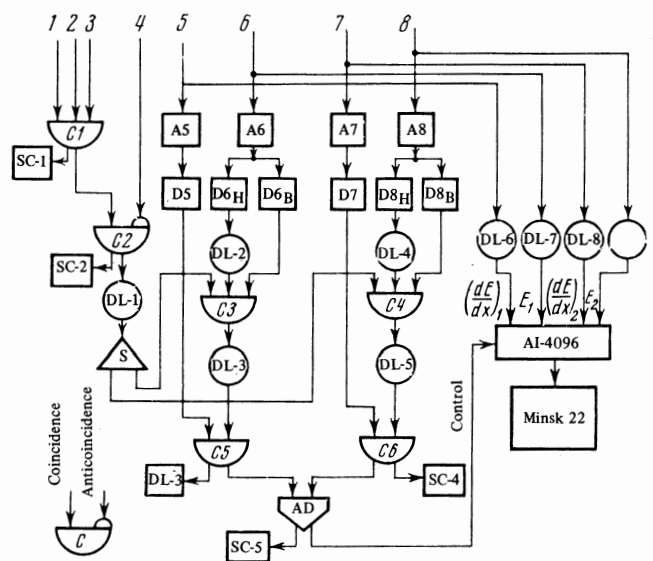


FIG. 2. Simplified block diagram of electronics: A—amplifier; D—discriminator; S—splitter; C—coincidence circuit; DL—delay line; AD—adder; SC—scaler; 1, 2, 3, 4, 5, 6, 7, 8—detectors.

<sup>1)</sup>Institute of Theoretical and Experimental Physics.

<sup>2)</sup>Erevan Physics Institute.

0.15–0.3 g/cm<sup>2</sup> were placed at an angle of 30° to the incident beam direction. We did not exclude the possibility of a large contribution from cases of simultaneous emission of two charged particles in a single pion-capture event,<sup>[6]</sup> and therefore counter 4, which helped identify cases of pion stopping in the target, was separated from it by 10 cm. This avoided possible distortions of the spectra as the result of strong suppression of the contribution from simultaneous emission of two charged particles. Counter 4 had the shape of a disk (diameter 8 cm, thickness 0.5 cm).

The charged particles emitted were analyzed by two telescopes consisting of counters 5 and 6 and 7 and 8, which were located at 180° to each other and at right angles to the pion beam. Counters 5 and 7 were silicon surface-barrier detectors of area 5.3 cm<sup>2</sup> and thickness 200 μ. These counters were used to measure the ionization loss  $dE/dx$  of the charged particles. Each counter was placed in an individual evacuated enclosure with thin polyester windows. Counters 6 and 8 were spectrometers employing CsI(Tl) crystals and served to measure the total energy  $E$  of the charged particles. Both crystals were cylindrical with a diameter 4 cm and height 3 cm. The energy resolution of the spectrometers was 11% for <sup>60</sup>Co γ rays. The number of particles passing through the target (circuit C1) was used as a beam monitor. Pion stoppings (1234) were identified by coincidence circuit C2. Emission of charged particles was identified by circuits C3 and C5 (123456 coincidences) or by circuits C4 and C6 (123478 coincidences).

An independent two-dimensional spectrum (energy and ionization loss) of the events from each telescope was recorded by means of a multidimensional AI-4096 analyzer of the Measurement Center, Laboratory of Nuclear Problems.<sup>[7]</sup> Triggering of the analysis system was accomplished by an adder Σ. In this way the information from the two telescopes was recorded in the analyzer memory simultaneously, regardless of which of them triggered the analyzer. The experiment was carried out on-line with a Minsk-22 computer.

## ANALYSIS OF RESULTS

In Fig. 3 we have shown as an illustration a two-dimensional spectrum of events recorded by one of the telescopes from carbon nuclei. The axes represent the values of energy  $E$  and ionization loss  $dE/dx$ . It is apparent that all points are concentrated in three zones corresponding to protons, deuterons, and tritons. One of the mass spectra is shown in Fig. 4. The abscissa is the value of the product  $E dE/dx$ . There is a small number of events (not shown in the figure) beyond the triton peak. It appears to us that they may be interpreted as passage through one telescope simultaneously of two charged particles (pp, pd, and so forth).

After separation of the charged particles according to mass, individual reconstruction of their total energy was carried out: account was taken of energy loss in the target, in the polyester windows, and in the semiconductor detector. It was verified that the light yields of a CsI(Tl) crystal on bombardment by protons, deuterons, and tritons are the same.<sup>[8]</sup> The accuracy of calibration of the energy scale in the present experiment was 10%. The energy spectra obtained from the

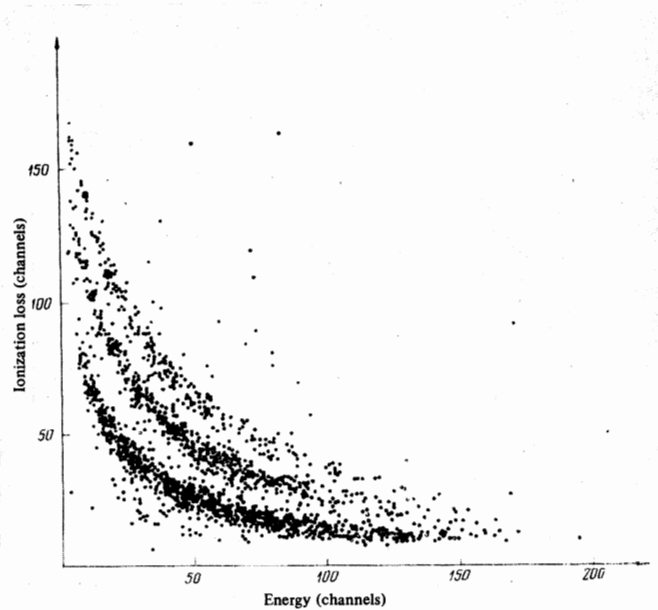


FIG. 3. Distribution of charged particles as a function of ionization loss and total energy for <sup>12</sup>C.

two telescopes in a given target were added. In measurements without a target, the effect dropped by about five times. The residual is due to stopping of pions in the plastic counter 3, the material enclosing it, and the air in front of counter 4. In determination of the relative yield of charged particles as a function of the nuclear charge, the stopping power of each target was taken into account. Cases of simultaneous emission of two charged particles were selected by the computer.

## EXPERIMENTAL RESULTS

The measured energy spectra of protons (p), deuterons (d), and tritons (t) are given in Tables I, II, and III. The events were summed over 3-MeV intervals. The errors shown are statistical. Table IV gives the normalization coefficients  $K$  by which the spectra are multiplied to be quantitatively comparable with each other. Figure 5 shows as an example the energy spectra of protons, deuterons, and tritons obtained in <sup>32</sup>S. The lower limit of the measured energy spectra is due to the thickness of the targets and silicon detectors.

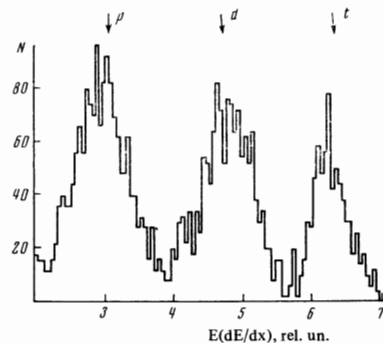


FIG. 4. Mass spectrum of charged particles for <sup>9</sup>Be.

Table I. Proton energy spectra

Target E, MeV	Be	C	Al	S	Ca	Cu	Cd	Pb
14	97±13	181±17	172±15	339±21	369±23	323±19	199±16	105±13
17	64±12	174±16	146±14	324±21	265±18	213±16	160±14	69±11
20	83±12	193±17	133±14	265±19	208±16	193±15	152±14	122±13
23	70±12	167±15	125±13	197±17	187±15	144±14	139±13	51±10
26	68±11	143±15	127±13	185±16	185±15	130±13	128±13	65±11
29	60±11	146±12	98±12	173±16	141±13	116±12	111±12	81±11
32	72±11	139±14	114±13	191±16	152±14	118±12	111±12	56±9
35	63±11	135±14	97±12	140±14	132±13	122±12	105±12	53±10
39	60±10	121±13	93±12	136±14	104±12	114±12	103±11	66±10
41	44±9	113±13	95±11	119±13	107±12	84±11	69±10	56±9
44	48±9	112±13	76±10	115±13	95±11	77±10	85±11	61±10
47	50±9	90±12	55±9	109±13	72±10	78±10	81±10	58±9
50	35±8	102±12	59±9	107±12	83±10	81±10	60±9	41±8
53	50±9	110±12	58±9	90±12	88±11	60±9	68±9	39±8
56	41±8	96±11	59±9	109±12	70±10	63±9	54±8	53±9
59	33±8	83±11	66±9	83±11	62±9	60±9	53±8	35±7
62	40±8	65±10	52±8	83±11	68±9	53±8	45±8	29±7
65	27±7	59±9	44±8	77±10	49±8	45±8	59±8	28±7
68	18±6	46±8	42±8	78±10	44±8	30±6	39±7	31±7
71	27±7	60±9	34±7	65±9	46±8	25±6	37±7	21±6
74	30±7	49±8	28±6	44±8	34±7	29±6	43±7	20±6
77	13±5	45±8	30±6	58±9	18±5	39±7	32±6	16±5
80	12±5	31±7	21±6	40±7	32±6	23±6	27±6	12±5
83	11±5	31±7	15±5	40±7	21±5	16±5	19±5	5±4
86	12±4	22±5	15±5	19±5	22±5	16±4	26±5	12±4
89	7±4	10±4	19±5	25±6	18±5	14±4	24±5	9±4
92	5±3	10±4	16±4	20±5	12±4	12±4	11±4	9±4
95	5±3	7±3	9±4	21±5	7±3	10±3	13±4	10±4
98	2±2	6±3	6±3	17±4	8±3	7±3	7±3	2±1
>100	12±4	25±6	25±7	38±8	14±3	10±3	28±8	19±5

Table II. Deuteron energy spectra

Target E, MeV	Be	C	Al	S	Ca	Cu	Cd	Pb
17	76±10	118±12	72±9	91±11	76±10	55±9	59±9	28±7
20	76±10	111±12	57±9	68±10	78±10	60±9	47±8	40±8
23	91±11	115±12	53±9	93±11	60±9	45±8	30±7	28±7
26	69±9	103±10	52±8	97±11	46±8	38±7	49±8	11±6
29	72±9	95±11	51±8	69±10	38±7	49±8	54±8	30±7
32	54±9	91±11	62±9	60±9	55±8	49±8	31±7	32±7
35	66±9	78±10	40±7	66±10	48±8	55±8	37±7	22±6
38	50±8	78±10	48±8	52±9	45±8	45±8	28±6	10±5
41	50±8	87±10	33±7	61±9	49±8	37±7	38±7	19±6
44	53±8	81±10	30±6	51±9	54±8	43±7	30±6	23±6
47	56±8	67±8	36±7	40±8	33±7	32±6	25±6	14±5
50	50±8	63±9	20±6	51±8	23±6	27±6	23±6	10±5
53	38±7	60±8	16±5	38±8	36±7	32±6	19±5	5±4
56	46±8	43±8	25±6	30±7	30±6	27±6	26±6	14±5
59	35±7	28±6	19±5	29±7	23±8	24±6	25±6	19±5
62	30±6	34±7	27±6	29±7	18±5	19±5	27±6	17±5
65	25±6	33±7	20±5	21±6	27±6	18±5	12±4	16±5
68	17±5	21±6	15±5	24±6	12±4	20±5	10±4	9±4
71	18±5	15±5	7±4	20±5	15±5	14±4	18±5	9±4
74	12±4	22±5	9±4	19±5	14±4	11±4	8±4	10±4
77	16±4	13±4	7±3	7±4	6±3	1±2	11±4	11±4
80	6±3	14±4	16±4	10±4	12±4	7±3	10±4	5±2
83	14±4	7±3	6±3	6±3	4±2	6±3	7±3	8±3
86	6±3	10±3	3±2	10±3	6±3	14±4	8±3	4±2
89	3±2	8±4	5±3	5±3	7±3	8±3	6±2	3±2
92	4±2	8±3	2±2	5±3	4±2	2±1	4±2	3±2
93	3±2	3±2	1±1	3±2	2±1	8±3	3±2	1±1
98	4±2	7±3	3±2	9±3	1±1	4±2	2±1	1±1
>100	5±2	10±3	18±4	14±4	2±1	8±2	9±3	12±3

Table III. Triton energy spectra

Target E, MeV	Be	C	Al	S	Ca	Cu	Cd	Pb
23	44±8	68±9	14±5	28±7	17±5	23±6	9±4	16±5
26	58±9	61±9	13±5	10±6	18±5	16±5	18±5	7±4
29	48±8	47±8	13±5	12±6	7±4	14±5	10±4	17±5
32	40±7	44±7	10±4	15±6	11±5	10±4	18±5	8±4
35	41±7	42±7	15±5	11±5	8±4	10±4	10±4	14±5
38	29±6	29±6	7±4	10±5	18±5	13±4	15±4	6±4
41	43±7	21±6	11±4	8±4	10±4	7±4	11±4	13±4
44	38±7	37±7	10±4	20±5	8±4	12±4	9±4	7±4
47	36±7	29±6	11±4	14±5	4±3	15±4	10±4	5±3
50	27±6	22±6	10±4	8±4	9±5	9±4	1±1	5±3
53	18±5	19±6	10±4	9±4	6±3	9±4	6±3	5±3
56	14±4	25±6	6±3	8±4	13±4	11±4	3±2	7±3
59	8±4	13±4	3±2	5±3	1±2	5±3	6±3	12±4
62	10±4	18±5	3±2	3±3	3±2	3±2	3±2	4±2
65	4±2	3±2	2±2	2±2	2±2	7±3	1±1	7±3
68	6±3	7±3	8±3	2±1	1±1	2±1	6±3	5±3
71	2±1	8±3	1±1	1±2	2±2	3±2	4±2	1±1
74	2±2	5±2	1±1	1±2	4±2	1±1	2±1	2±1
77	1±2	1±1	1±1	5±3	4±2	5±2	2±1	2±1
>80	7±3	10±3	10±3	9±3	11±4	10±4	6±2	9±4

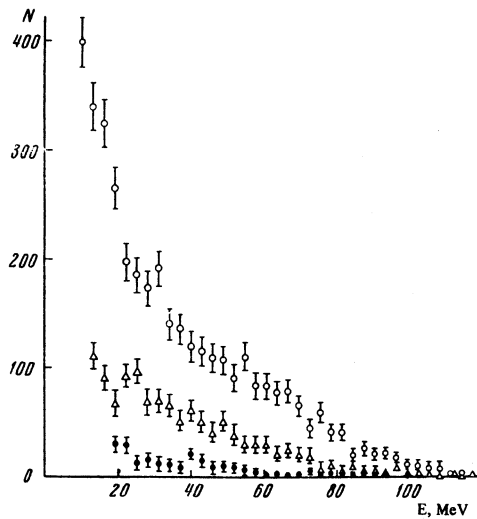


FIG. 5. Energy spectra of protons, deuterons, and tritons obtained in capture of pions by  $^{32}\text{S}$  nuclei:  $\circ$ —protons,  $\Delta$ —deuterons,  $\bullet$ —tritons.

Figures 6–8 show the relative integral probabilities of emission of p, d, and t for various threshold energies as a function of nuclear charge. For ease of interpretation the corresponding experimental points are connected by the smooth curves. The errors shown in the figures are due to the statistics and to the uncertainty in the number of pion stoppings in the target. Figure 9 shows the fractions of p, d, and t in the total number of charged particles with energies above 24 MeV, as a function of nuclear charge.

## DISCUSSION OF RESULTS

Figure 10 shows the energy spectra of charged particles from pion capture in carbon. It is necessary to allow for the fact that the proton spectra above 100 MeV are strongly attenuated as a result of the thickness of the CsI(Tl) crystals used. The solid points were taken from the work of Vaisenberg et al.<sup>[2]</sup> They are plotted together with ours in the region 50–80 MeV. The solid curves in the figure were calculated by Kolybasov<sup>[9]</sup> on the assumption of an  $\alpha$ -particle pion-capture mechanism. The dashed curves show the phase-space distributions. The experimental and theoretical spectra have been normalized to the same area. It is easy to see that the proton spectra in the figure disagree substantially. This indicates that the  $\alpha$ -particle mechanism cannot be the only mechanism in pion capture.

The experimental spectrum of deuterons is consistent with the theoretical spectrum within experimental error. The agreement of the measured triton spectrum with the calculated spectrum indicates a major role of the  $\alpha$ -particle mechanism of pion capture.<sup>[10]</sup> It should be noted that the agreement permits only the phase-space calculations to be discarded in this case.

For energies above 15 MeV, the relative proton yield as a function of nuclear charge (Fig. 6) has a peak at  $^{40}\text{Ca}$ . It is interesting to note that Castleberry et al.,<sup>[4]</sup> working with  $^{40}\text{Ca}$ , also obtained a maximum yield of protons with energies above 6 MeV, although with larger errors. Unfortunately, these authors do not report yields for other threshold energies, which makes

FIG. 6. Integral probability for proton emission  $W_p$  as a function of nuclear charge.

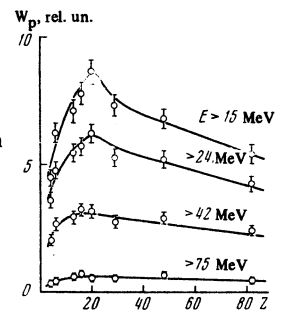


FIG. 7. Integral probability of deuteron emission  $W_d$  as a function of nuclear charge.

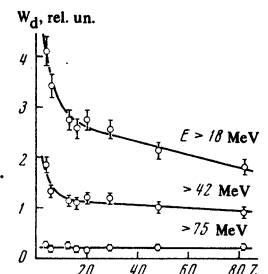


FIG. 8. Integral probability of triton emission  $W_t$  as a function of nuclear charge.

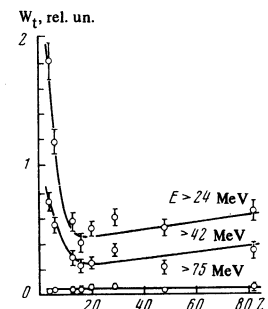
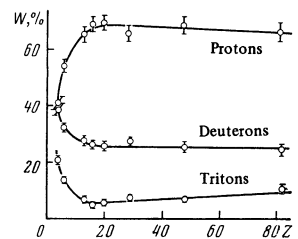


FIG. 9. Relative yields of protons, deuterons, and tritons,  $W$  in per cent as a function of nuclear charge for energies above 24 MeV.



it difficult to compare their results qualitatively with ours. However, the maximum in the proton yield of  $^{40}\text{Ca}$  found by Castleberry et al.<sup>[4]</sup> is expressed more sharply than in our case. This is explained by the fact that the peak is due mainly to low-energy protons. At higher energies the proton yield depends only weakly on nuclear charge. We wish to call attention to the fact that in our earlier work,<sup>[5]</sup> in which we measured energy spectra of charged particles from capture of stopped negative muons by nuclei, a similar dependence was obtained for the integral probability of proton emission with a maximum at  $^{40}\text{Ca}$ .

The relative yields of deuterons and tritons (Figs. 7 and 8) first fall sharply with increasing nuclear charge and then remain constant within experimental error. The relative fractions of protons, deuterons, and tritons

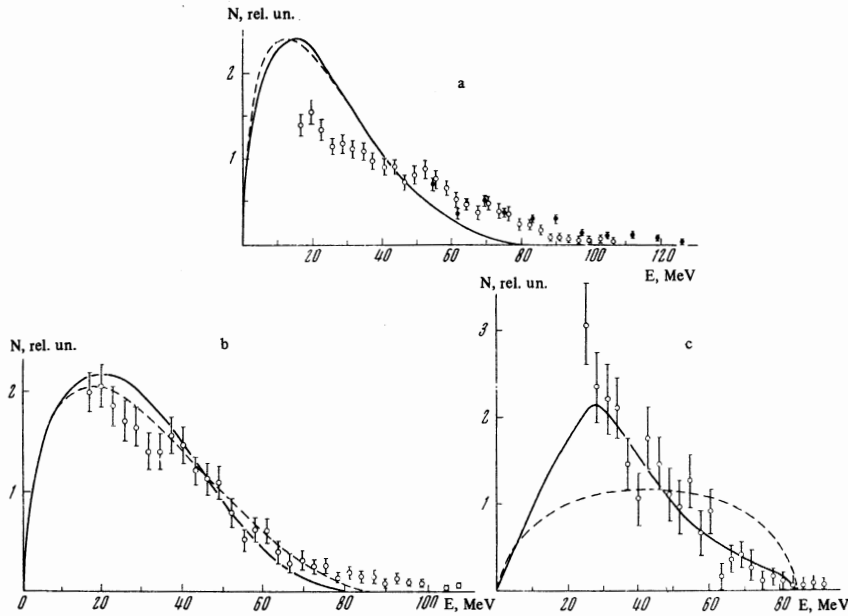


FIG. 10. Energy spectra of protons (a), deuterons (b), and tritons (c) from pion capture in <sup>12</sup>C. The solid curves correspond to the  $\alpha$ -particle mechanism, and the dashed curves to phase space.

in the total number of charged particles for energies above 24 MeV (Fig. 9) also change substantially only for small values of nuclear charge. At high energies the dependence on nuclear charge disappears. Similar results were obtained previously<sup>[5]</sup> with muons.

Because of the small solid angles subtended by the semiconductor detectors at the target (1%), we were unable to obtain good statistics on cases of simultaneous detection of two charged particles. For an energy of each particle of at least 24 MeV, about ten such events were recorded during the entire bombardment. During the same time about 2500 events were recorded in the single-particle spectrum. If it is true that at 0°, i.e., in one telescope, we are correctly separating events with participation of two charged particles simultaneously, the number of such events with a total energy of at least 50 MeV is close to the number of events with simultaneous detection of two particles with at least 24 MeV each and an angle between them of 180°. On this basis, although it is not completely justified, we can suggest that, in cases of simultaneous emission, the charged particles are distributed isotropically with respect to each other. Then, if we take into account the stipulations made above, for light nuclei the number of pion-capture events with simultaneous emission of two charged particles ( $E > 24$  MeV each) is approximately equal to the number of capture events with emission of one particle ( $E > 24$  MeV). It may be recalled that the probability of emission of a high-energy proton in a pair with a neutron amounts to 40% of the total probability of proton emission.<sup>[11]</sup>

The contribution of simultaneous emission of two charged particles is small in heavy nuclei. In this con-

nection it is interesting to note that "heavy" pairs (dd, dt, tt) are preferentially emitted from light nuclei, and with increasing nuclear charge, lighter pairs (pp, pd) begin to predominate.

It is apparent that further study of negative-pion capture with simultaneous emission of two high-energy charged particles will help to clarify the capture mechanism.

In conclusion the authors express their deep gratitude to A. O. Vaisenberg, V. M. Kolybasov, T. I. Kopaleishvili, A. I. Mukhin, V. I. Petrukhin, and R. A. Éramzhyan for helpful discussions, and also to V. V. Fil'chenkov and I. A. Yutlandov for assistance in this work.

<sup>1</sup>A. O. Vaisenberg, É. D. Kolganova, and N. V. Rabin, Zh. Eksp. Teor. Fiz. **47**, 1262 (1964) [Sov. Phys. JETP **20**, 854 (1965)].

<sup>2</sup>A. O. Vaisenberg, N. V. Rabin, and V. F. Kuzichev, Yad. Fiz. **11**, 48 (1970) [Sov. J. Nucl. Phys. **11**, 26 (1970)].

<sup>3</sup>V. S. Demidov, V. S. Verebryusov, V. G. Kirillov-Ugryumov, A. K. Ponosov, and F. N. Sergeev, Zh. Eksp. Teor. Fiz. **46**, 1220 (1964) [Sov. Phys. JETP **19**, 826 (1964)].

<sup>4</sup>P. J. Castleberry, L. Coulson, R. C. Minehart, and K. O. H. Ziock, Phys. Lett. B **34**, 57 (1971).

<sup>5</sup>Yu. G. Budyashev, V. G. Zinov, A. D. Konin, A. I. Mukhin, and A. M. Chatrchyan, Zh. Eksp. Teor. Fiz. **60**, 19 (1971) [Sov. Phys. JETP **33**, 11 (1971)].

<sup>6</sup>P. Ammiraju and L. M. Lederman, Nuovo Cimento **4**, 283 (1956).

<sup>7</sup>A. N. Sinaev, A. A. Stakhin, and N. A. Chistov, JINR preprint 13-4835, Dubna, 1969.

<sup>8</sup>Yu. G. Budyashov, V. G. Zinov, A. D. Konin, A. I. Mukhin, and A. M. Chatrchyan, JINR Report R1-5682, Dubna, 1971.

<sup>9</sup>V. M. Kolybasov, Yad. Fiz. **3**, 729 (1966) [Sov. J. Nucl. Phys. **3**, 535 (1966)].

<sup>10</sup>T. I. Kopaleishvili and I. Z. Machabeli, Yad. Fiz. **12**, 525 (1970) [Sov. J. Nucl. Phys. **12**, 286 (1971)].

<sup>11</sup>M. E. Nordberg, Jr., K. F. Kinsey, and R. L. Burman, Phys. Rev. **165**, 1097 (1968).

Table IV

Target	Be	C	Al	S	Ca	Cu	Cd	Pb
K	4.2	3.6	4.0	2.6	3.7	3.7	3.6	4.7